$H^2(d,\gamma)He^4$, in agreement with the value of 0.1 μb obtained by Fowler *et al.*[25] at 1.2 Mev.

A 70-kev thick helium gas target was bombarded with 1055-kev deuterons (energy at center of target). This bombarding energy would form Li^6 in the first excited level at 2.187 Mev.[26] No gamma radiation was detected from this level, and an upper limit of 0.1 mb was sent on the cross section for the reaction $He^4(d,\gamma)Li^6$.

A 200-kev thick oxygen gas target was bombarded with 1100-kev deuterons (energy at center of target), the energy required to form F^{18} in the 8.5-Mev excited state.[27] Again no capture gamma rays were detected, and an upper limit of 0.5 mb was set on the cross section for the reaction $O^{16}(d,\gamma)F^{18}$.

[25] Fowler, Lauritsen, and Tollestrup, Phys. Rev. **76**, 1767 (1949).
[26] Browne, Williamson, Craig, and Donahue, Phys. Rev. **83**, 179 (1951).
[27] G. Brubaker, Phys. Rev. **56**, 1181 (1939).

PHYSICAL REVIEW VOLUME 93, NUMBER 5 MARCH 1, 1954

Charged Particles from the Interaction of 14-Mev Neutrons with Li^6 and Li^7†

GLENN M. FRYE, Jr.
University of California, Los Alamos Scientific Laboratory, Los Alamos, New Mexico
(Received November 24, 1953)

The angular distribution of the charged particles produced in the bombardment of Li^6 and Li^7 by 14-Mev neutrons was observed with nuclear emulsions in a multiplate camera. Metallic targets of enriched Li^6 and Li^7 were used. The following cross sections were measured: $Li^6(n,p)He^6$, 6±2 mb; $Li^6(n,d)He^5$, 89±10 mb; $Li^6(n,d)He^{5*}$, 77±9 mb; $Li^6(n,t)He^4$, 26±4 mb; $Li^7(n,t)He^5$, 55±8 mb. The reaction $Li^7(n,d)He^6$ was also observed but was not well enough resolved to give an angular distribution and total cross section. No evidence was found for the formation of He^7 by $Li^7(n,p)He^7$ with a cross section greater than 5 mb in the range $-1.0>Q>-7.0$ Mev. The angular distributions obtained for $Li^6(n,d)He^5$ and $Li^6(n,d)He^{5*}$ indicate these reactions proceed mainly by an inverse stripping or pick-up process. The energy spectrum of the neutrons from $Li^6(n,d)He^5(n)He^4$ and $Li^6(n,d)He^{5*}(n)He^4$ is calculated using several assumptions for the angular distribution of the He^5 disintegration.

I. INTRODUCTION

THE interaction of neutrons with Li^6 has been studied by many investigators,[1] particularly for neutron energies of 2.5 Mev and below, where only the well-known $Li^6(n,t)He^4$ reaction is energetically possible. Recently Ribe[2] has measured this cross section as a function of energy from 0.88 to 14.2 Mev. Roberts and co-workers[3] have obtained the angular distribution of the tritons for energies up to 2 Mev using Li^6 loaded nuclear track plates. For the other charged particle reactions, Poole and Paul[4] used the formation of 0.8-sec He^6 to establish the $Li^6(n,p)He^6$ reaction for neutrons from 4 to 12 Mev. By the activation technique Battat and Ribe[5] measured the cross section for this reaction at 14.1 Mev as 6.7±0.8 mb. Also at 14 Mev Ribe[6] detected a comparatively large group of deuterons and obtained a value of ~200 mb for the cross section. For Li^7 the $Li^7(n,d)He^6$ process has been observed,[5] again by the activation of He^6, with a cross section at 14.1 Mev of 9.8±1.1 mb.

The present experiment was undertaken to determine the angular distributions of the various charged particle groups and their total cross sections at 14 Mev. The above reactions were observed, and angular distributions obtained except for $Li^7(n,d)He^6$. In addition tritons from $Li^7(n,t)He^5$ were found. The deuterons observed in the Li^6 experiment were established to be due to two broad groups, $Li^6(n,d)He^5$ and $Li^6(n,d)He^{5*}$. The deuteron angular distribution showed the mechanism to be predominately a pick-up process.[7]

II. EXPERIMENTAL PROCEDURE

A. Multiplate Camera and Collimator

The experimental arrangement, shown in Fig. 1, was similar to that used previously by Allred, Armstrong, and Rosen[8] for *n-p* and *n-d* scattering. 14-Mev neutrons were furnished by the *d*-T reaction in which the 250-kev diatomic deuteron beam from the Los Alamos Cockcroft-Walton accelerator was used to bombard a tritium-zirconium target. The neutron flux was monitored by counting the accompanying alpha

† Work performed under the auspices of the U. S. Atomic Energy Commission.
[1] See F. Ajzenberg and T. Lauritsen, Revs. Modern Phys. **24**, 321 (1952), and Hornyak, Lauritsen, Morrison, and Fowler, Revs. Modern Phys. **22**, 291 (1950) for complete references to the earlier work.
[2] F. L. Ribe, Phys. Rev. **91**, 462 (1953).
[3] Darlington, Haugsnes, Mann, and Roberts, Phys. Rev. **90**, 1049 (1953); J. H. Roberts (unpublished report).
[4] M. J. Poole and E. B. Paul, Nature **158**, 482 (1946).
[5] M. E. Battat and F. L. Ribe, Phys. Rev. **89**, 80 (1953).
[6] F. L. Ribe, Phys. Rev. **87**, 205 (1952) and private communication.
[7] S. T. Butler, Proc. Roy. Soc. (London) **A208**, 559 (1951); S. T. Butler and E. E. Salpeter, Phys. Rev. **88**, 133 (1952).
[8] Allred, Armstrong, and Rosen, Phys. Rev. **91**, 90 (1953).

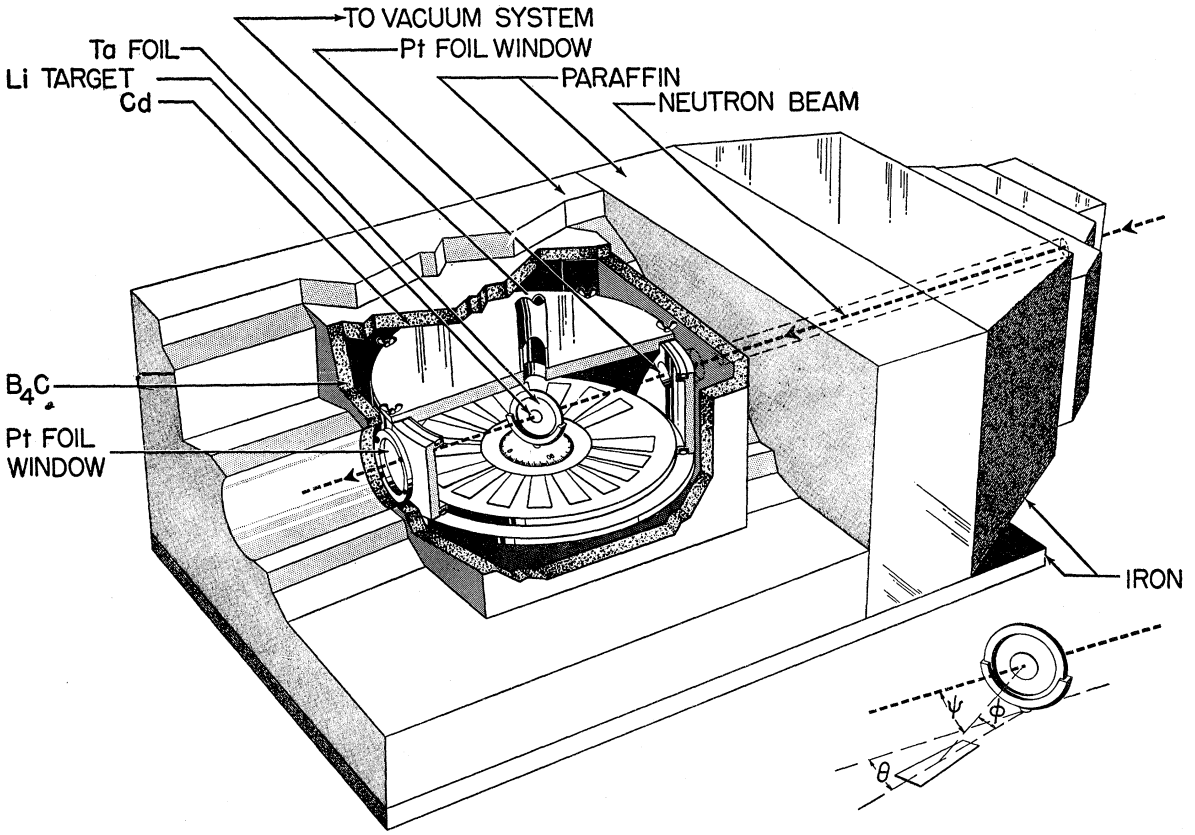

FIG. 1. Perspective view of collimator, multiple camera, and shielding.

particles from the d-T reaction. 18 in. of iron and 8 in. of paraffin in a collimator of approximately pyramidal shape shielded the plates from the source. A cylindrical channel in the iron, $\frac{3}{4}$ in. in diameter, gave a beam 1 in. in diameter at the target. The camera was also shielded by a 1-in. layer of boron carbide powder and a sheet of 0.030-in. cadmium. This was necessary because of the large $Li^6(n,t)He^4$ cross section for low-energy neutrons.

In the camera the plates lay in a plane $1\frac{1}{8}$ in. below the axis of the beam with their inner edges on a circle of radius 3 in. The inset of Fig. 1 shows the target-plate geometry in detail. ϕ is the angle between the plane of the plate and the line from the center of the target to the center of the plate area analyzed. θ is the azimuthal angle between the axis of the plate and the projection of the beam axis upon the plane of the plates. From ϕ and θ one may immediately calculate ψ, the laboratory angle between the neutron beam and particle direction. In this particular geometry, values of ψ from 11° to 169° could be obtained. The plane of the target foil was such that it made an angle of 45° with the beam. Two targets, placed back-to-back, could be used simultaneously. The one facing the collimator will be referred to as the back target and the other as the forward target. The camera was lined with 0.010-in. gold foil to minimize charged-particle production in the walls.

Figure 2 shows the spectrum of the neutron beam which was obtained by measuring the proton recoils from a paraffin target.[8] Figure 2(a) is the spectrum resulting from measurements at a laboratory angle of 15°, while Fig. 2(b) is an average over fifteen angles from 15° to 40°. In each case the intensity of degraded neutrons (1.5 to 12 Mev) is approximately 3 percent of the 14-Mev flux.

B. Single Plate Camera

To obtain data at angles less than 11° a single plate camera was used (Fig. 3). With this arrangement there is no shielding, and the plate is exposed directly to the neutron source. The tracks due to particles coming from the Li target originate on the surface of the emulsion and thus may be distinguished from the much greater number of proton recoils which start within the emulsion. In practice it was found that a neutron flux of $10^9/cm^2$ could be tolerated on the plate. A higher flux resulted in such a "thicket" of recoil tracks down in the emulsion that there was danger that a track originating on the surface could not be followed over its entire range. A typical arrangement was to have the target midway between the source and plate, 8 cm from each.

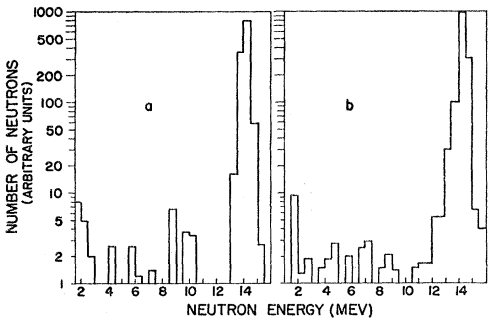

FIG. 2. Neutron spectrum at the target. (a) is the spectrum obtained from proton recoils at 15°. (b) is an average over fifteen angles from 15° to 40°.

C. Preparation of Targets

Metallic Li targets were prepared by vacuum evaporation from a tantalum vessel onto a 4-mil Ta foil. Li^6 and Li^7, enriched to 90.9 percent and 99.9 percent, respectively, were furnished by Oak Ridge. The vessel or oven was cylindrical in shape, having one end closed and the other end flared at 45°. This design confined the evaporation to a cone which gave a thicker target for a given charge in the oven and also helped to conserve the amount of separated isotope available. Heat was supplied by a tungsten coil wound on a lavite sleeve into which the oven fitted. The evaporated Li was cooled by circulating ice water behind the brass plate on which the Ta foil was mounted. A vacuum slide valve[9] between the oven and foil could be closed to separate them during outgassing. The pressure during evaporation was always $<10^{-5}$ mm of Hg. The closed valve and foil were detachable from the evaporating unit so that the foil could be transferred to a dry box without being exposed to air. If metallic Li is exposed to air, Li_3N is the first compound to form. Chemical analysis showed the amount of nitrogen contamination to be less than 0.5 percent by weight. Analysis of the data (see Fig. 4) showed that hydrogen was present to 0.3 percent in the 4-mg/cm² and 0.08 percent in the 10-mg/cm² Li^6 targets, indicating a layer of hydrogenous material. With this system it was possible to make a target having a surface density as great as 10 mg/cm² in one evaporation. Desiccated helium or argon circulated through the dry box kept the targets untarnished for several months. The targets were weighed by placing them in a light-weight (20-g) Al box with an O-ring seal to retain the helium atmosphere in the box and then using a Mettler gram-atic balance. This arrangement gave the Li weight to an accuracy of 1.5 percent.

Before the target could be placed in the camera, it was necessary to remove the water vapor from the plates by pumping on them for several hours with a liquid air trap in the vacuum system. A sealed container was devised so that the target could be placed in position in the center of the camera without breaking the seal. After pumping the plates the procedure for mounting the target was to fill the camera with argon, remove the camera lid, place the sealed container holding the target in the center of the camera, open and remove the container, replace the lid, and start the vacuum pump. This sequence prevented any air from contacting the Li. After completion of a run the procedure was reversed to recover the target. Upon examination in the dry-box, the targets appeared unchanged. The single plate camera could be loaded by placing it in the dry-box. It was necessary to use one Li^6 target (4 mg/cm²) whose surface had darkened slightly during preparation. Data obtained from this target were later compared with that from an untarnished one in the single plate camera. No variation outside that attributable to statistics was found between the two spectra.

Table I lists the various experimental runs which were made. Four runs were made with the multiplate

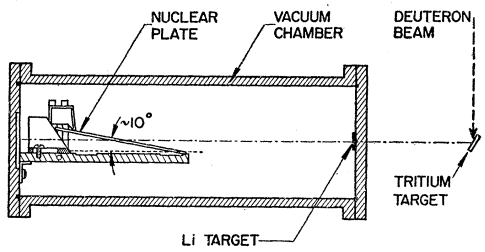

FIG. 3. Single plate camera.

[9] Wahl, Forbes, Nyer, and Little, Rev. Sci. Instr. 23, 379 (1952).

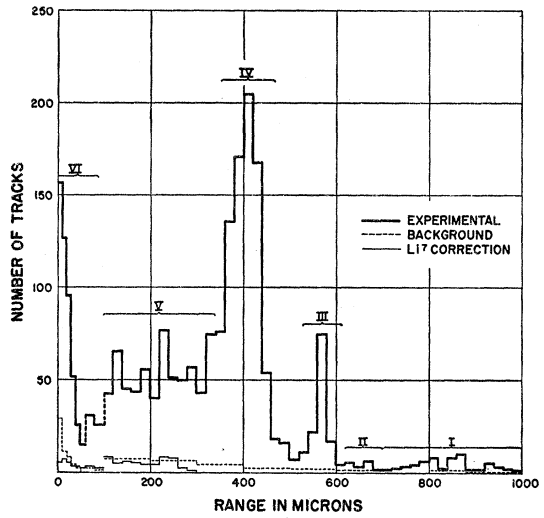

FIG. 4. Range analysis of charged particles produced by 14-Mev neutrons on Li^6 using the multiplate camera. The indicated particle groups are: I—recoil protons, II—$Li^6(n,p)He^6$, III—$Li^6(n,t)He^4$, IV—$Li^6(n,d)He^5$, V—$Li^6(n,d)He^{5*}$, VI—mostly alpha particles from $Li^6(n,t)He^4$, $Li^6(n,d)He^5(n)He^4$ and $Li^6(n,d)He^{5*}(n)He^4$. The data below 60μ are plotted in 10μ intervals; above 60μ in 20μ intervals. The tracks below 100μ came from the analysis of 0.36 cm² of plate; above 100μ from 1.32 cm² of plate.

camera. Two Li^6 targets were used having surface densities of 10 mg/cm² and 4 mg/cm², one Li^7 target of 7 mg/cm², and one background run with a bare Ta foil. Single plate camera runs were made with the same or similar targets. In run *L*-1 a Li^6 loaded plate was placed on the floor of the multiplate camera at the foot of the target holder to determine the number of Li^6 disintegrations produced by thermal and epithermal neutrons.

D. Analysis of the Plates

Ilford 200-μ *E*-1 plates were used except for runs *L*-2 and *L*-4 where 400-μ plates were necessary at laboratory angles of less than 30° to insure that no "good" tracks passed out the bottom of the emulsion. The plates were developed by the *A* and *B* solution cold technique.[10] The optical equipment was as described by Rosen[10] and length measurements of tracks longer than 100μ were made with the precision stage. In the analysis of the plates three measurements were made upon each track: (1) the projected length, i.e., the length in the plane of the emulsion, along the long axis of the plate, (2) the dip angle ϕ_0, and (3) θ_0, the angle between the projected length and the long axis of the plate. Using the experimentally determined shrinkage factor of 2.3 one may compute the true range of each track. Moreover, the angles ϕ_0 and θ_0 made it possible to determine whether or not the particle came from the Li target. Thus limits could be set on ϕ_0 and θ_0 to eliminate background tracks coming from other directions. A check on these criteria was provided by the fact that the number of tracks which lay outside these angular limits was the same with or without a Li target in the camera.

TABLE I. Experimental runs.

Run	Forward target	Backward target	Neutrons/cm² at target
	A. Multiplate camera		
L-1	Li^7: 6 mg/cm²	Li^6:10 mg/cm²	4.44×10^9
L-2	Li^6:10 mg/cm²	Li^7: 6 mg/cm²	4.68×10^9
L-3	Bare Ta foil	Li^6: 4.2 mg/cm²	5.83×10^9
L-4	Li^6: 4.2 mg/cm²	Bare Ta foil	5.84×10^9
	B. Single-plate camera		
Run	Target		Neutrons/cm² at target
L-5	Li^6: 7 mg/cm²		2.28×10^9
L-6	Li^7: 5.6 mg/cm²		2.28×10^9
L-7	Li^6:10 mg/cm²		3.98×10^9
L-8	Li^7: 5.6 mg/cm²		3.98×10^9

III. CORRECTIONS AND EVALUATION OF ERRORS

Figure 4 shows a typical range analysis for Li^6 taken at a laboratory angle of 17° with the multiplate camera. The various particle groups from Li^6 are indicated as well as the recoil protons from the hydrogen contamination in the target. Figure 5 shows a corresponding spectrum for Li^7 obtained at 0° with the single plate camera.

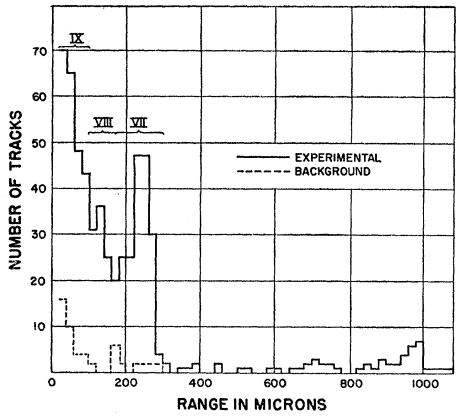

FIG. 5. Range analysis of charged particles produced by 14-Mev neutrons on Li^7 using the single plate camera. The indicated particle groups are VII—$Li^7(n,t)He^5$, VIII—$Li^7(n,d)He^6$, IX—partially due to alpha particles from $Li^7(n,t)He^5(n)He^4$. The data below 60μ are plotted in 10μ intervals; above 60μ in 20μ intervals.

The following corrections were applied to these data: (1) The background found with the blank Ta foil was subtracted. The magnitude of this background is indicated in Figs. 4 and 5. Since the number of background tracks was small, an average correction was applied over each 100μ interval (except for 0–100μ where 20μ steps were taken). At most the background amounted to a few percent of any particle group. (2) A correction was made for the tracks resulting from the hydrogen contamination in the target; for this a total *n-p* cross section at 14 Mev of 0.685 barn[11] was

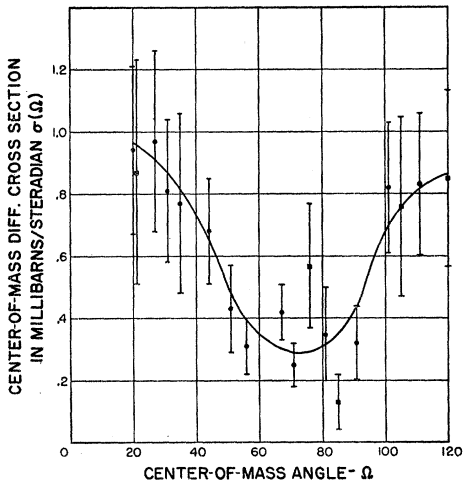

FIG. 6. Angular distribution of protons from $Li^6(n,p)He^6$. In Figs. 6, 7(a), 8, and 9 the crosses are single plate camera points, the squares are data from the 10-mg/cm² Li^6 target, the triangles are from the 4.2-mg/cm² Li^6 target, and the circles are an average of the data from the 10- and 4.2-mg/cm² targets.

[10] L. Rosen, Nucleonics **11**, No. 7, 32 (1953); **11**, No. 8, 38 (1953).

[11] Poss, Salant, Snow, and Yuan, Phys. Rev. **87**, 11 (1952).

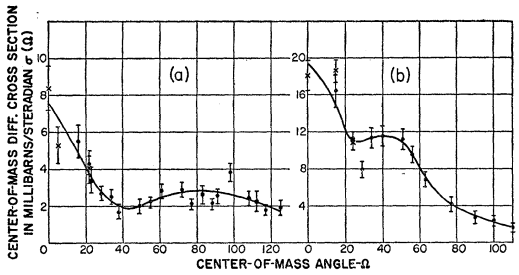

FIG. 7. Angular distribution of tritons from (a) $Li^6(n,t)He^4$ and (b) $Li^7(n,t)He^5$. In Fig. 7(b) the circles are from the 5.6-mg/cm² Li^7 target.

used and isotropic scattering in the center-of-mass system was assumed. Although this correction reduced the $Li^6(n,p)He^6$ and $Li^6(n,t)He^4$ differential cross sections by a maximum of 30 percent (at center-of-mass angles 29° and 49°, respectively), the total cross sections were reduced by less than 5 percent. The deuteron angular distributions were not affected. (3) Lower-energy neutrons present in the 14-Mev beam give triton tracks of the same range as the deuteron tracks produced by the 14-Mev neutrons. Use of Ribe's[2] data for the $Li^6(n,t)He^4$ cross section as a function of energy gives a 2-percent correction to the total deuteron cross sections. (4) The final Li^7 data may be used to correct for the Li^7 present in the Li^6 targets. Since the range of the tritons from Li^7 is less than 300μ, only the $Li^6(n,d)He^{5*}$ deuterons are affected. An average correction over 40μ intervals was applied, amounting at most to 10 percent. Its magnitude is indicated in Fig. 4.

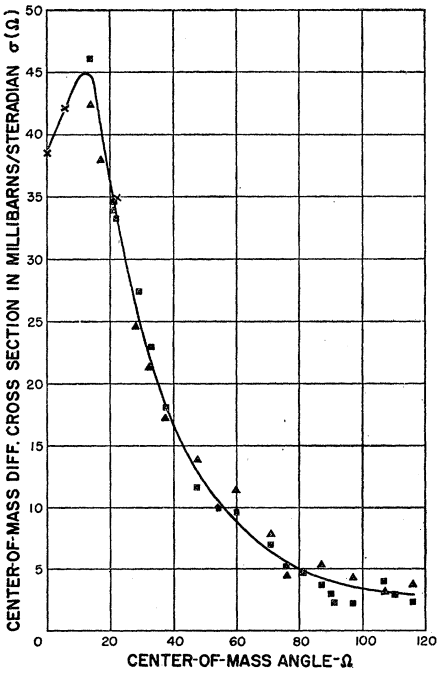

FIG. 8. Angular distribution of deuterons from $Li^6(n,d)He^5$ showing points from the various runs.

(5) Analysis of the number of Li^6 disintegrations in the Li^6 loaded plate enables one to correct the Li^6 data for the number of tracks of range 40μ and under produced by thermal and epithermal neutrons in the target.

In addition to the statistical error the following systematic errors were present: (1) Uncertainty in the neutron flux: 4 percent. (2) Determination of the number of Li atoms in the target: 1.5 percent. (3) Measurements of the camera geometry: 3 percent. (4) Uncertainty as to the exact limits of each particle group (Figs. 4 and 5). The separation between the two deuteron groups is admittedly arbitrary as is discussed further below. It is somewhat difficult to estimate the magnitude of this error for the other reactions as the separation between groups is a function of angle. However, it is felt that 7 percent represents an upper limit.

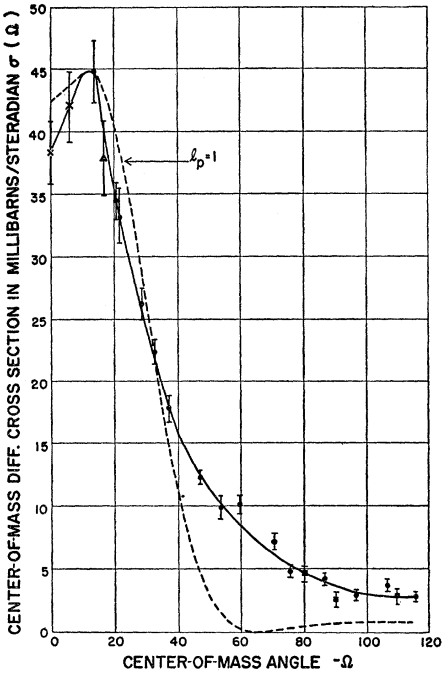

FIG. 9. Angular distribution of deuterons from $Li^6(n,d)He^5$. Here the averaged points and the statistical errors are shown. The solid curve is the same as Fig. 8. The dotted curve is a theoretical Butler curve for $l_p=1$; $r_0=4.5\times10^{-13}$ cm.

Only the statistical errors are shown on the angular distribution curves, Figs. 6–10. The errors on the total cross sections, Table II, include both the statistical and systematic contributions.

IV. RESULTS AND DISCUSSION

A. $Li^6(n,p)He^6$

An angular distribution was obtained for this reaction, Fig. 6, but in view of the poor statistics all that can be said is that there is an asymmetry with a minimum near 70°. The total cross section is 6±2 mb, in good agreement with Battat and Ribe's[5] value of 6.7±0.8 mb.

B. $Li^6(n,t)He^4$

Figure 7 illustrates the triton angular distribution. This single forward maximum is in contrast to the lower-energy data[3] which have maxima at both 0° and 180°. The total cross section is 26±4 mb.

C. $Li^6(n,d)He^5$

There was some question as to whether the group of tracks from 340 to 500μ in Fig. 4 was due to deuterons from $Li^6(n,d)He^5$ or protons from $Li^6(n,p)He^{6*}$, as formation of the 1.71-Mev level[1] in He^6 would give protons of approximately this range. One method of identification was to vary the neutron energy and measure the corresponding change in range of the group. This was done by using the atomic beam of the Cockcroft-Walton at 250 kev which will give 14.8-Mev neutrons at 0° to the deuteron beam and 13.5-Mev neutrons at 150°. Although these neutrons are not monoenergetic, due to the thick tritium-zirconium target employed, the shift in range of this group may be measured relative to the shift of the triton group. The results indicated that the group was predominately deuterons.

TABLE II. Total cross sections.

Reaction	Total cross section in millibarns
$Li^6(n,p)He^6$	6±2
$Li^6(n,t)He^4$	26±4
$Li^6(n,d)He^5$	89±10
$Li^6(n,d)He^{5*}$	77±9
$Li^7(n,t)He^5$	55±8

A more sensitive method of particle identification was the grain counting of individual tracks. For a plate exposed in the single plate camera one had 14-Mev recoil proton tracks in the emulsion and triton tracks from the known triton group for calibration of the grain density characteristics of the emulsion. Moreover, grain counting of recoil protons at various emulsion depths gave a check on uniformity of development. From counting 60 tracks it was found that in the range interval 500–340μ approximately 95 percent of the tracks were deuterons, and in the interval 340–160μ approximately 90 percent of the tracks were deuterons. Below 160μ it was not possible to make positive identification of the tracks. Since the percentage of tracks not identified as deuterons was of the same order as the background, it was assumed for purposes of calculating the angular distribution and total cross section that the two groups of tracks identified in Fig. 4 as $Li^6(n,d)He^5$ and $Li^6(n,d)He^{5*}$ were entirely deuteron.

The separation point for the two deuteron groups was rather arbitrarily taken as the range at which the intensity of the ground state deuterons fell to that of the lower-energy group. The minimum deuteron range was set by the range where alpha particles from $Li^6(n,t)He^4$ would appear. Thus the width of the lower-energy

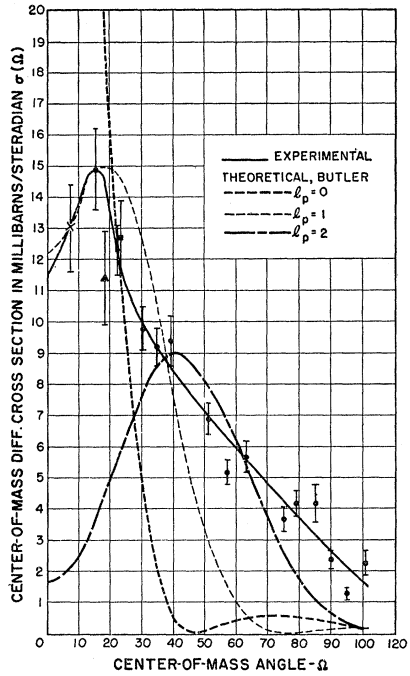

FIG. 10. Angular distribution of deuterons from that part of $Li^6(n,d)He^{5*}$ where $Q=-4.3$ to -6.7 Mev. The dashed curves are Butler curves for $l_p=0$, 1, 2; $r_0=4.5\times10^{-13}$ cm.

deuteron group is a function of the angle and the group so defined cannot be used as such to obtain an angular distribution. However the total cross section given in Table I for $Li^6(n,d)He^{5*}$ does include all the deuterons with ranges lying between the minimum deuteron range from $Li^6(n,d)He^5$ and the maximum alpha particle range from $Li^6(n,t)He^4$.

Figure 8 shows the angular distribution for $Li^6(n,d)He^5$. The good agreement among the various runs provides a check on the foil weighing and flux measurement techniques, and on the different geometries used in the single and multiplate cameras. The theoretical curve shown in Fig. 9 is for an inverse stripping or pick-up process, calculated using Butler's theory[7] for the inverse reaction $He^5(d,n)Li^6$. By the principle of detailed balancing this should give the angular distribution of $Li^6(n,d)He^5$. Fairly good agreement, especially for small angles, is obtained for

$$r_0=4.5\times10^{-13}\text{cm};\quad l_p=1.$$

Thus there should be a change in parity between He^5 and Li^6 and a spin change of $\frac{1}{2}$ or $\frac{3}{2}$, which is consistent with the usual assignments to He^5 of $^2P_{\frac{3}{2}}$ and Li^6 of $^3S_1$.[1,12] The total cross section for $Li^6(n,d)He^5$ is 89±10 mb, considerably larger than the $Li^6(n,p)$ or $Li^6(n,t)$ cross sections. This favoritism for the emission of the loosely bound deuteron is difficult to explain by a compound nucleus model and provides further evidence for the reaction proceeding by a pick-up mechanism.

[12] D. R. Inglis, Revs. Modern Phys. 25, 390 (1953).

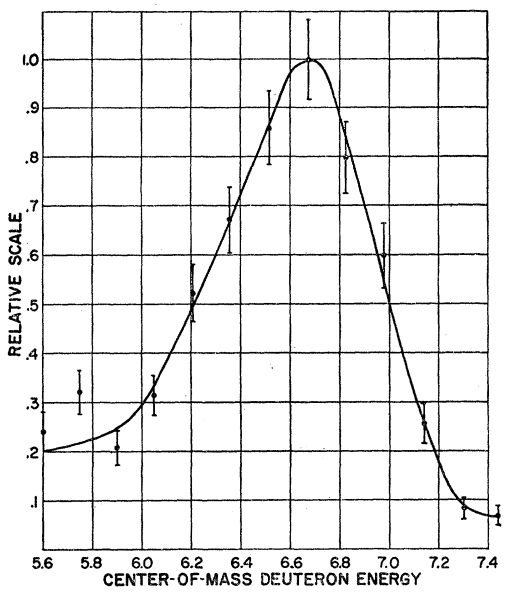

FIG. 11. Shape of the deuteron peak from $Li^6(n,d)He^5$ in the center-of-mass system.

Although the deuterons below 320μ appear to be a continuum rather than a discrete group, it was decided to take the tracks from 320–200μ, which correspond to a $Q=-4.3$ to -6.7 Mev, and treat them as if they were a fraction of a very broad group. (This was the largest fraction that could be taken without including alpha particle tracks from $Li^6(n,t)He^4$ at larger angles.) The resulting angular distribution is shown in Fig. 10. Its shape is similar to the angular distribution of the ground state deuterons. Again the Butler curve[7] for $l_p=1$ seems to give the best fit, although the quantitative agreement is not as good as for $Li^6(n,d)He^5$. If the procedure of using only part of this broad group to determine the angular distribution is valid, the fit for $l_p=1$ is consistent with the result obtained from the analysis of n-He^4 scattering;[13,14] i.e., above the ground state of He^5 lies a very broad $P_{\frac{1}{2}}$ level. Since a fairly sharp level, i.e., one having about the same width as the ground state, had been reported in He^5 at 2.6 Mev,[15] a special search was made in this region (275μ in Fig. 4) using the data from several runs, but no deuteron peak ascribable to this level was seen.

A value for the ground-state energy of He^5 and its width could be found by comparing the peak from $Li^6(n,d)He^5$ with the triton group from $Li^6(n,t)He^4$ for which a $Q=4.780$ Mev has been well established.[1] For this purpose the plate at 17° laboratory angle from run L-3, where the 4-mg/cm^2 target was used, was analyzed over 1.32 cm^2 in an effort to obtain improved statistics. When one obtains the deuteron energy by comparison with the triton energy, only a relative range energy curve for nuclear emulsions is necessary. Also, errors in the target thickness and geometry cancel out, at least in the first approximation. In this manner it was found that the Q for the $Li^6(n,d)He^5$ reaction is -2.57 ± 0.10 Mev or, using the mass table of Li *et al.*,[16]

$$He^5=He^4+n+1.09\pm0.10 \text{ Mev}.$$

It was found that the half-width of the triton group could be explained entirely by the following experimental factors: (1) Target thickness, 0.43 Mev; (2) angular resolution, 0.29 Mev; (3) range straggling in the plate, 0.19 Mev; (4) range measurement errors, 0.05 Mev; and (5) thick target neutron source, 0.05 Mev, giving an rms half-width of 0.5 Mev compared to the experimental value of 0.5 ± 0.1 Mev. When applied to the deuteron group, the same calculation gave a half-width of 0.39 Mev compared to the observed value of 1.10 Mev. After removing the experimental contribution, one obtains a nuclear half-width for the deuteron group in the center-of-mass system of 0.8 Mev. Figure 11 shows the shape of this deuteron group in the center-of-mass system.

D. Energy Spectrum of Neutrons from $Li^6(n,d)He^5(n)He^4$ and $Li^6(n,d)He^{5*}(n)He^4$

Since the He^5 formed in these deuteron reactions has a lifetime only a little longer than the nuclear transit time, the He^5 at once breaks up into He^4 and a neutron. From the observed energy spectrum of the deuterons at

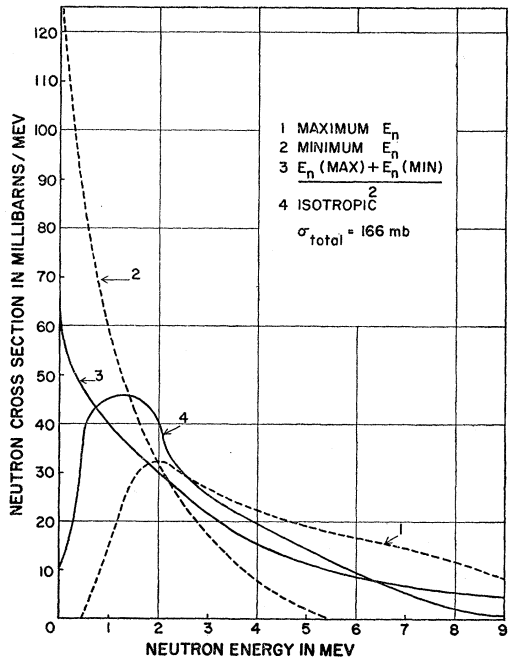

FIG. 12. Neutron energy spectrum from $Li^6(n,d)He^5(n)He^4$ and $Li^6(n,d)He^{5*}(n)He^4$.

[13] D. C. Dodder and J. L. Gammel, Phys. Rev. **88**, 520 (1952).
[14] R. K. Adair, Phys. Rev. **86**, 155 (1952).
[15] W. T. Leland and H. M. Agnew, Phys. Rev. **82**, 559 (1951).
[16] Li, Whaling, Fowler, and Lauritsen, Phys. Rev. **83**, 512 (1951).

each angle, the angular and energy distribution of the He^5's may be calculated. Then if an assumption is made about the angular distribution of the disintegration $He^5 \rightarrow He^4 + n$, the energy spectrum of the neutrons may be calculated. Four different assumptions were made:

(1) The neutron is emitted in the same direction as the He^5 motion. This delta-function angular distribution gives the largest number of high-energy neutrons.

(2) The neutron is emitted in the opposite direction to the He^5, giving the largest number of low-energy neutrons.

(3) Half the neutrons are emitted as in (1) and half as in (2), an approximation to an angular distribution peaked forward and backward in the He^5 center-of-mass system.

(4) The He^5 breakup is isotropic in the He^5 center-of-mass system. The neutron energy distributions resulting from these various assumptions are given in Fig. 12.

Of course (1) and (2) are highly artificial assumptions. The true energy distribution is probably given by (3) or (4) or some combination of them.

E. $Li^7(n,t)He^5$

The angular distribution of this reaction, Fig. 7, is similar to the triton distribution from Li^6. The total cross section is 55 ± 8 mb.

F. $Li^7(n,d)He^6$

This reaction was observed at laboratory angles up to 30° but was not well enough resolved to enable its angular distribution or total cross section to be determined.

G. Other Possible Reactions

The spectrum from Li^6 shows a number of tracks below 100μ which presumably are the result of alpha particles accompanying the triton and deuteron reactions. In addition there may be deuterons of range less than 100μ. To test this possibility the short tracks were integrated over all angles to give a total cross section which should equal the sum of the cross sections for the triton and deuteron groups, 192 mb. A minimum range was set on the short tracks so that no Li recoils, which may have a range of 15μ, would be counted. The resulting cross section for short tracks was 140 mb, indicating no large deuteron cross section below 100μ. That the alpha cross section is less than the deuteron plus triton cross section may be attributed to some of the alphas having an initial range less than the Li^7 recoil range and others being reduced in range below this minimum by energy loss in the target.

The same type of analysis may be applied to the Li^7 data. Below the triton group one should have alphas coming from the breakup of the accompanying He^5. If one subtracts the 9.8-mb cross section[5] for $Li^7(n,d)He^6$ one finds a cross section of 161 mb for the shorter tracks, of which the $Li^7(n,t)He^5 \rightarrow He^4 + n$ alphas can account for 55 mb. There are four other reactions which could produce charged particles of this range:

(1) $Li^7(n,t)He^{5*}(n)He^4$ $\quad Q > -6.6$ Mev

(2) $Li^7(n,n')Li^{7*}(t)He^4$ $\quad Q > -6.6$ Mev

(3) $Li^7(n,2nd)He^4$ $\quad Q = -8.72$ Mev

(4) $Li^7(n,3np)He^4$ $\quad Q = -10.95$ Mev

(4) is barely above threshold. A knowledge of the $(n,2n)$ cross section would enable one to set an upper limit to (3). Possibly (1) and (2) are the most likely since they have the highest Q and the smallest number of particles involved. If all the short tracks were due to (1) and (2) the cross section would be ~ 50 mb.

H. Search for He^7

To investigate the possibility of the formation of He^7 by the reaction $Li^7(n,p)He^7$, a search was made of the Li^7 data for such a group of protons. Since none was found, the cross section for the formation of He^7 is ≤ 5 mb for $-1.0 > Q > -7.0$.

ACKNOWLEDGMENTS

The author would like to thank the entire microscope group for the analysis of the plates, Mrs. J. Gammel and Mrs. L. Stewart for help in the calculations, Mrs. M. Downs for typing the manuscript, Dr. J. Coon, Mr. R. Davis and Group *P*-4 for use of the Cockcroft-Walton facilities, Dr. A. H. Armstrong and Dr. J. C. Allred for assistance during the experimental runs, and, especially, Dr. Louis Rosen for many helpful discussions.